15TH IEA HEAT PUMP CONFERENCE
MAY 26–29, 2026 | HOFBURG
VIENNA 2026
DECARBONISATION THROUGH INNOVATION

HP2035: Performance Assessment of Natural Refrigerants in Heat Pumps for Micro-district Heating

P. Peikani[a,b*], M. Lauermann[a], B. Windholz[b], H. Madani Larijani[a,b], S. Sawalha[b]

[a]Austrian Institute of Technology (AIT), Center for Energy, 1210 Vienna, Austria,
[b]KTH Royal Institute of Technology, Department of Energy Technology, 114 28 Stockholm, Sweden

Abstract

Residential heating is a major contributor to final energy consumption and emissions in the EU. As the EU strives to meet carbon neutrality goals by 2050, improving the efficiency and sustainability of residential heating systems is a critical priority. Transitioning to low-carbon technologies, such as heat pumps and district heating networks, is essential for reducing emissions, enhancing energy security and improving resource efficiency. Conventional district heating networks often rely on flue gas heat recovery from combustion plants, and decentralized heat pump systems that use ambient air as heat source can suffer from reduced efficiency in cold or fluctuating climates. The deployment of heat pumps into micro-district heating networks can be a viable solution to mitigate these challenges, particularly by utilizing local heat sources to maximize system efficiency under cold ambient conditions. Dual-source heat pump can dynamically combine heat sources, such as ambient air and urban waste heat, to enhance seasonal performance, and reduce compressor work during peak demand. This study investigates the seasonal performance of a dual-source heat pump system in a micro-district heating using natural refrigerants.
The study compares the performance of natural refrigerants, low-GWP alternatives aligned with EU regulatory frameworks, with conventional HFC-based systems. A numerical simulation was conducted to assess the system's behavior under varying ambient conditions and heating demands. Results demonstrate that dual-source configuration enhance system efficiency under low ambient temperature, and natural refrigerants can outperform conventional HFC-based systems in practical scenarios. Including a secondary heat source improved the COP up to 30%. Ammonia exhibited the highest SCOP. While the dual-source configuration introduces additional complexity, The outcomes highlight performance improvement at lower temperatures and suggest strong potential for future applications in urban heating networks. This study contributes to ongoing decarbonization efforts and encourages further development and integration of dual-source systems within future micro-district heating networks.

Keywords: Dual-source Heat Pums, Natural Refrigerant, Micro-District Heating;

1. Introduction

The European Union is likely to fall behind with achieving the desired 2050 carbon neutrality goal in terms of reducing both direct and indirect CO_2 emissions. In 2023, households accounted for 26% of the EU's final energy consumption [1]. Within the residential sector, space heating and domestic hot water demand together represent over 70% of this consumption. This substantial proportion shows the importance of prioritizing emission reduction and energy transition strategies in the residential sector [1].

In 2023, natural gas was a major energy carrier for space heating and domestic hot water across the EU, with 34% and 39% of the consumed energy, respectively [1]. The path to decarbonization of heating and cooling in residential buildings is to replace fuel-based heating systems with technologies that facilitate the integration of renewable energy through sustainable solutions, such as district heating networks.

District heating production accounted for approximately 10% of the global final heating demand in buildings and industry in 2023, holding a 13% market share in Europe. Projections suggest that district heating (DH) could expand its market share in Europe up to 50% by 2050 [2], driven by the growing emphasis on

* Corresponding author. *E-mail address:* pantheia.peikani@ait.ac.at

15th IEA Heat Pump Conference 2026 - THN1.1 - https://doi.org/10.23697/1ve8-4q80

energy security, decarbonization, and energy efficiency. DH remains a key strategy for lowering carbon emissions. By centralizing heat production, it reduces reliance on individual heating systems, diversifies heat supply sources, and enables flexibility to switch between them based on availability and cost.

However, the widespread adoption of DH faces several challenges [3], including high installation costs, regulatory uncertainties, and insufficient integration with other energy sectors. Currently, 90% of global heating demand for DH is derived from carbon-intensive fossil fuels [4]. Additionally, traditional 3rd generation district heating (3GDH) systems often operate at high temperatures, making them less energy efficient and retrofitting existing systems to lower temperatures poses a major technical challenge [5].

In response to these challenges, Micro-District Heating (MDH) systems are emerging as a key solution for residential decarbonization. They bridge the gap between individual building heat pumps and large centralized district heating systems, offering a sustainable and cost-effective alternative to traditional high-temperature district heating. MDH systems flexibly integrate low-temperature heat sources, such as ambient air and local waste heat, to provide heating and cooling to residential buildings. Urban excess heat is in close vicinity to demand side [6] and faces several inherent limitations when considered for direct use in large DH networks [7]. Conventional European district heating networks require a minimum source temperature around 70 °C and only a share of 42% is supplied by renewable and waste heat sources [8]. Deployed at the neighborhood scale, MDH systems provide a flexible and scalable solution, particularly suited to densely populated urban areas with space constraints. This integration directly addresses technical barriers related to source-demand proximity and allows for more manageable investment sizes, alleviating concerns about high upfront capital expenditure. However, the successful implementation of MDH systems depends on addressing the technical challenges of efficiently integrating multiple heat sources into a unified system that can adapt to fluctuating temperatures throughout the year. The potentials and constraints of different heat sources used in heat pump systems have been investigated in various studies. It has been demonstrated that the seasonal performance factor (SPF) of heat pumps is directly correlated with the temperature of the heat source. While MDH presents a promising alternative, key questions remain about how to select and integrate multiple heat sources often at different temperature levels within a neighborhood to optimize heat pump performance.

The successful implementation of MDH systems could fundamentally transform the heating infrastructure of cities. By grouping buildings into flexible, low-temperature networks, they allow neighborhoods to be capable of balancing local supply and demand. This shift toward localized heating networks creates a demand for integrating advanced heating technologies that can efficiently make use of heat that would otherwise go to waste.

The state-of-the-art development in multi-source heat pumps mainly aimed at supporting the decarbonization of heating systems and improving energy efficiency by utilizing various heat sources in large-scale heat pump applications. Multi-source heat pumps can overcome the limitations of single-source heat pumps by combining two or more heat sources at different temperature levels.

Air source heat pumps (ASHPs) are widely used due to their ease of installation, but their efficiencies are strongly influenced by ambient air temperature. When outdoor temperatures drop, the efficiency of ASHP decreases, making them less suitable for cold climates, particularly when the heat demand is high. Ground source heat pumps (GSHPs) offer higher annual performance and better stability than ASHPs, but they have high investment costs due to required space and drilling depth. The combination of ground and air source heat pumps are developed to overcome the limitations of relying on a single heat source [9] and to reduce the effects of short-term temperature fluctuations. The ground-air dual source heat pumps enable smaller borehole size and offer lower drilling cost compared to conventional GSHPs [10].

Solar energy is frequently integrated into heat pump systems to boost efficiency and utilize renewable energy sources. In some systems, solar thermal collectors are installed in series with ground heat exchangers [11]. Solar heat is also used to thermally recharge the ground during the cooling season, mitigating the performance degradation due to thermal imbalance when the ground is only used as a heat sink [12]. The intensity of solar radiation fluctuates throughout the day therefore it introduces an intermittent and unstable heat flux. A significant challenge for solar thermal integration is the offset between seasonal availability and demands. Hence, the application of solar heat pumps in cold climate requires a large collector area, which will lead to a high initial investment, relatively high capital cost and installation difficulties.

Several studies have demonstrated the reliability and energy-saving potential of multi-source systems [13], [14], [15], [16]. It was demonstrated that implementing dual-source heat pump for meeting heating and cooling demands in residential buildings, can reduce annual electricity consumption by 22%. When combined with time-of-use tariffs, the system can chieve electricity cost savings of 48% compared to conventional air-source heat pumps [16]. With regards to the operation of multi-source heat pumps combined with thermal storage, the effects of user-side parameters and ambient temperature were investigated in a system integrating a CO_2 air-source heat pump and a ground-source heat pump with a thermal storage tank. The system exhibited reduced sensitivity to ambient temperature fluctuation, and a 69% reduction in CO_2 emissions [14].

Another study demonstrated that incorporating a second waste heat source at an intermediate temperature can improve heat pump performance depending on the system configuration. A system with R410A as refrigerant using closed economiser with vapor injection showed limited improvements due to the compressor's inability to handle large refrigerant injections at intermediate pressure. In contrast, a dual-compressor configuration with proper oil management successfully achieved the desired performance, with up to 35% increase in COP and heating capacity when the second heat source was around 20 °C [15]. Previous experimental work has investigated a dual-source heat pump prototype with two independent compressors in a parallel configuration for both air and ground heat sources and R454B as refrigerant. It was demonstrated that, at an ambient temperature -7 °C, the required cooling load on both heat sources was reduced by 41% and 58%, respectively, compared to ground- and air-source systems. This allows for a potential reduction in installation space and drilling depth of the ground source heat exchanger, as well as a reduction in fan speed. The study highlighted some key technological challenges posed by the parallel operation of two compressors, including cycle stability, which is affected by fluctuating expansion valves, and compressor oil shift, which can cause lubrication issues [17].

The key principle of a multi-source heat pump is to use heat sources at different temperatures within the system, through which the heat from the second source is often introduced at an intermediate pressure level. The main challenges in dual-source heat pumps, especially those operating with parallel heat sources, is high complexity in the refrigerant cycle, which impose limitations on operational conditions. Therefore, further research is needed to better understand how the temperatures of different heat sources affect overall performance and efficiency.

The challenge of selecting refrigerants with minimal environmental impact is critical for the sustainability and long-term viability of heat pump technologies in MDH systems. The refrigerant choice directly influences both the direct emissions through GWP, and indirect emissions through system efficiency of the heat pump system, making it crucial for determining overall environmental performance. The EU's F-gas regulation mandates a phase-down of refrigerants with high global warming potential (GWP) and prohibits the use of certain refrigerants in new refrigeration equipment. In response, hydrofluoroolefin (HFO) refrigerants with lower GWP levels were introduced to the market and have been widely adopted by manufacturers. However, these substances have subsequently been found to degrade into trifluoroacetic acid (TFA), a persistent and potentially harmful compound. Consequently, many HFOs are included in EU proposals to restrict them due to their link to per- and polyfluoroalkyl substances (PFAS), which could lead to a ban or limitation of their use in the future.

Despite strong system-level progress in residential-scale heat pumps such as low-charge designs, there is limited comparative analysis of refrigerant performance specifically for heat pumps in MDH networks, which operate at medium scale and supply temperatures below 80 °C. In this paper, a systematic thermodynamic evaluation was performed on a heat pump cycle for heating in a MDH network comprising cluster of apartment blocks. The proposed system utilizes ambient air and local urban excess heat, with the ability to operate on multiple sources simultaneously and prioritize sources to maintain higher system efficiency. Selected natural refrigerants are employed as the working fluid, and their competitiveness is evaluated against HFCs in terms of delivering high performance and meeting the required thermal demand. The heat pump cycle is modeled to assess seasonal performance and to determine optimal operating parameters under varying conditions over the year. Furthermore, the influence of different working fluids on system performance is investigated across two-source cycle configurations to identify the most viable design alternatives.

2. Methodology

2.1. System-Level Analysis

A system-level analysis was conducted to characterize the heating demand of nine existing residential apartment buildings, as well as the operational conditions of the proposed heat pump, within a representative micro-district heating (MDH) network in Vienna, Austria. City Energy Analyst (CEA) [18] was used to estimate the annual thermal energy demand for space heating and domestic hot water preparation in apartment buildings. Figure 1 shows the total heat demand profile for one year, at the coldest week of the year, and the coldest days in January and December. The load profiles show that heating demand consistently follows outdoor temperature, and highest loads occur during the coldest periods. The analysis considered the buildings' construction year and renovation rate, which define their thermal performance and insulation characteristics.

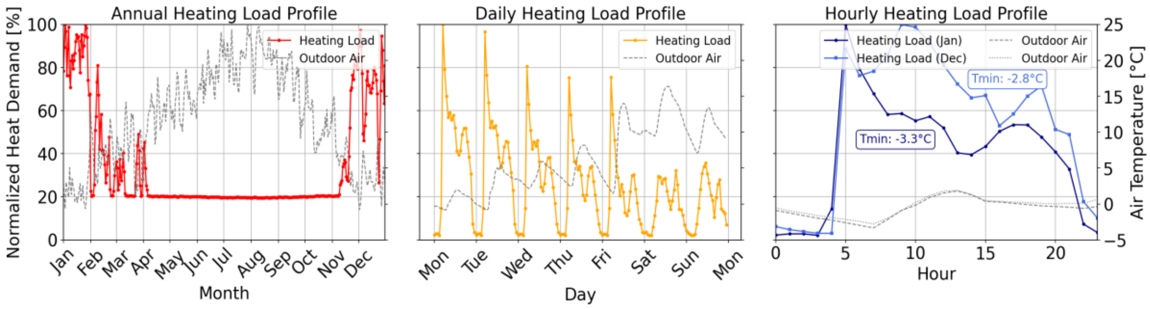

Figure 1 Normalized heating demand of the micro-district heating network at various timescales

The CEA simulations provided time series data for the heating demand, as well as the supply and return temperature profiles for the MDH network. The simulated apartment cluster is located in Vienna and is presented in Figure 2 (left). Based on the required heating load for the proposed heating network for the apartment cluster, the nominal capacity of the heat pump was determined to cover 99% of the of the total annual heating energy demand (kWh), as shown in Figure 2 (right). This corresponds to a 265 kW heat pump, which has the capacity to cover around 60% of the peak demand.

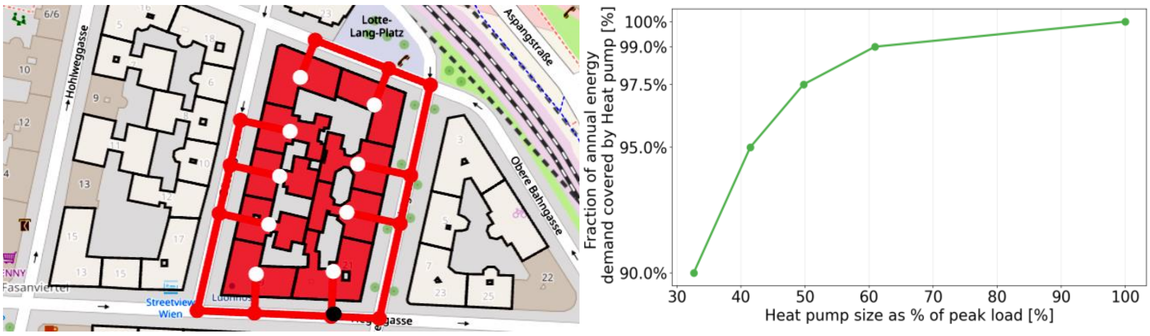

Figure 2 Overview of supply system map of MDH network for apartment cluster in Vienna (left), heat pump size (right)

The inputs for the heat pump model are the operational flow temperature and the heat load distribution in the sink side under varying outdoor temperature conditions. To establish the boundary conditions for the subsequent thermodynamic cycle simulations, the heat demand profile and heating characteristic curves, were derived by correlating the required heating capacity of the MDH and working temperature with the outdoor temperature.

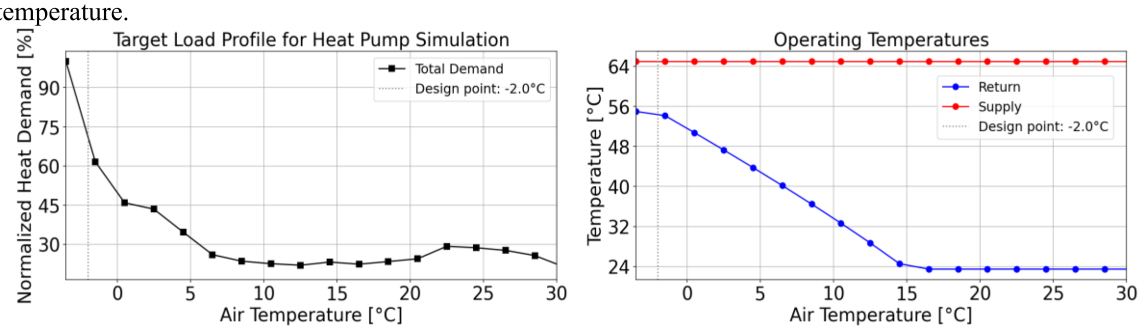

Figure 3 Normalized heat demand (left) and, supply/return temperature profiles (right) for heat pump model

The total heat demand profile in Figure 3 (left) was generated by first grouping the hourly outdoor air temperatures from the Vienna weather file in 2020 into 1 K intervals. Then, each temperature bin was associated with its cumulative occurrence in hours and the corresponding heating-degree hours below the upper outdoor temperature limit of 15 °C for space heating. The resulting dataset provided the frequency distribution of outdoor conditions over the year and the corresponding thermal weighting factors for space heating and domestic hot water. These weighting factors were then used to aggregate the hourly demand data into representative temperature bins to generate the target load profile of for the heat pump model at different ambient temperatures according to EN 15316-4-2 [19].

The correlation provided in [19] Annex B was used to correlate the return temperature with outdoor temperature for different emission systems, as shown in Figure 3 (right). For this study, the curve corresponding to a radiator-based emission system in an average climate was used. This curve was determined by linear interpolation between the design point (corresponding to the design outdoor temperature) and the upper operating limit (heating cut-off temperature). A modulation factor of n = 1.3 was applied to represent the response characteristics of the radiator emitter system.

2.2. System Definition and Boundary Conditions

The heat pump modeling process begins with establishing the boundary conditions and operational parameters required for system. The reference system is an air-source heat pump (ASHP). Following the analysis of reference configuration, a dual-source heat pump (DSHP) was modeled to represent the potential integration of a low-temperature heat source available in urban area, as shown in Figure 4 . The DSHP comprises two parallel evaporators, each connected to an independent heat source. Evaporator 1 operates at low pressure, and it is coupled to ambient air. Temperature variations in Evaporator 1 follow the local bin distribution. Evaporator 2 is connected to a secondary source (above 0 °C) at intermediate pressure, representing urban waste heat. Both evaporators are linked to parallel compressors, which enable flexible operation and simultaneous heat extraction from both sources, depending on temperature and availability.

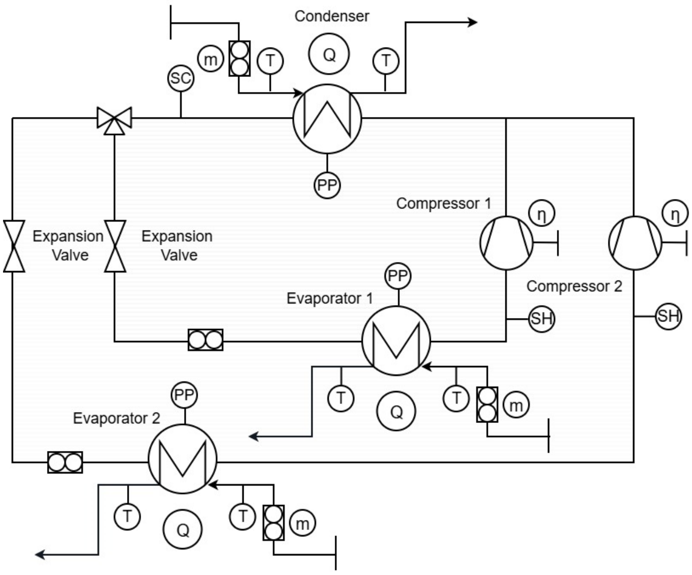

Figure 4 Schematic of the DSHP configuration

The boundary conditions include external system requirements and internal design assumptions. The MDH supply temperature is fixed at 65 °C. The system uses two heat sources. The first is an air source with a variable ambient temperature, which accounts for seasonal variations. The second is a brine source, which represents secondary heat sources at relatively stable temperatures. The examined temperature conditions of 0 °C, 5 °C, 15 °C, and 25 °C reflect typical heat source temperatures in urban environments without seasonal fluctuations [20], [21]. Examples of these sources include:

- Sewage systems in high-density urban areas, which have temperatures between 8 °C and 25 °C and show low daily variations
- Water bodies, such as seas, lakes, or rivers, which have temperatures between 4 °C and 11 °C and exhibit minimal seasonal changes due to their high heat capacity
- Groundwater, which has stable temperatures between 10 °C and 12 °C
- Near-surface geothermal probes and collectors, which have temperatures between −5 °C and 20 °C.
- Data centers, which provide relatively constant temperatures throughout the year.

For both heat sources, a fixed temperature difference of 5 K is assumed between the inlet and outlet.

The system is modeled under steady-state conditions. The compression processes are assumed to be adiabatic, and a constant isentropic efficiency of 70% is assigned to the compressor. The expansion process through the valve is assumed to be isenthalpic, and component volumes are neglected. For simplicity, the model neglects secondary losses, such as pressure drops in the heat exchangers and pipelines, as well as heat dissipation to the environment.

Regarding design parameters, the minimum pinch-point temperature difference between the refrigerant and the heat source/sink within the condenser and evaporator is fixed at 3 K. This value subsequently determines the required UA-value [kW/K] of the heat exchanger. When designing heat exchangers, it is important to strike a balance between the surface area of the heat exchanger and the improvement in system performance. This balance can be better understood by using a fixed pinch point temperature difference for all refrigerants [22]. The evaporator outlet superheat is set to 7 K to ensure dry compression, and the condenser outlet subcooling is fixed at 5 K.

Table 1 Simulation Inputs

Category	Variable	Unit	Value
Setpoint Variables	$T_{sink,\mathrm{out}}$	°C	65
	$T_{sink,\mathrm{in}}$	°C	55 … 25
	$T_{source,in}$	°C	-3.5 … 30
Boundary Conditions	Superheating	K	7
	Subcooling	K	5
	Pinch Point Temperature	K	3
Actuating Variable	$\dot{V}_{swept}$	m³/h	PI → $\dot{Q}_h^{design}$

2.3. Key Performance Indicators

System performance was primarily assessed using the coefficient of performance (COP_1). COP_1 measures the ratio of the useful heating capacity delivered to the heat sink to the total electrical power input required by the heat pump (in this case only the compressor(s)). The seasonal coefficient of performance (SCOP) accounts for temporal variations in air temperature and evaluates average system efficiency over a year. SCOP reflects the influence of temperature fluctuations in the heat source on the overall heating performance over time.

The heat source ratio (β) was used to quantify the contribution of the second heat source relative to the total heat supplied by both evaporators [23].

$$\beta = \frac{\dot{Q}_{evap2}}{\dot{Q}_{evap2} + \dot{Q}_{evap1}} \tag{1}$$

The β value in Eq. (1), which ranges from 0 to 1, represents different operating scenarios. A β value of 0 indicates operation with only the air heat source active, while $\beta = 1$ corresponds to full utilization of the second heat source with the air source inactive. The setpoint input for the PI controller of each compressor covers a portion of the heating capacity supplied to the condenser by adjusting the RPM of the compressor. To ensure combined operation of the evaporators during the year, a limiting threshold was implemented so that no more than 70% and no less than 30% of the heating load is covered by either heat source. The influence of different intermediate source temperatures on the heat pump performance was analyzed. Comparing refrigerants based on thermodynamic performance offers a useful measure of their overall behavior, particularly when considering energy efficiency alongside investment-related indicators such as volumetric cooling capacity and UA values. Such comparisons are also less sensitive to assumptions in the modeling [22]. Previous findings [24] showed that the environmental effect of additional components in more complex configurations can be negligible as long as the cycle efficiency improves.

3. Results and Discussion

A comparison of thermophysical properties was carried out among six refrigerants to evaluate the feasibility and theoretical potential of natural refrigerants under the defined operating conditions, as compared to a reference HFC refrigerant R410A, as shown in Table 2. The molar mass of a refrigerant affects its density and heat of vaporization. An important property is the vapor pressure at design operating point, to ensure that the system operates within acceptable pressure limits, avoiding both sub-atmospheric conditions and excessively high pressures. Natural refrigerants have lower vapour densities than the reference HFC refrigerant due to their lower vapor pressure. At a given temperature, a higher vapor pressure and lower normal boiling point is favourable, because they indicate effective heat absorption at lower source temperatures and help maintain a lower pressure ratio in the heat pump system. Some refrigerants (e.g., R600 and R600a) have relatively higher normal boiling point which makes them to be suitable for specific operating conditions. A higher latent heat of vaporization implies a greater heat transfer capability and better heat absorption on the source-side, as well as a smaller required refrigerant mass flow rate for the same heating output. Ammonia has the lowest vapor density and the highest latent heat of vaporization. The cycle evaluation was performed based on the method in [25] with a reference condensation temperature of 50 °C and an evaporation temperature of -20 °C. Hydrocarbons, such as propane, are highly flammable (A3), whereas ammonia is classified as mildly flammable and toxic (B2L). Using these substances in heat pumps for micro-district heating systems as low-GWP alternatives to HFCs requires additional precautions and safety considerations regarding flammability and toxicity. EN 378 [26] establishes maximum allowable refrigerant charges based on access categories of spaces and location classifications of equipment. Although no charge restrictions apply to open-air locations or machinery rooms, safety considerations are necessary to prevent refrigerant leaks from endangering people or property.

Table 2 Thermophysical properties and specifications of refrigerants

	Safety Class	M kg/kmol	T_{NBP} °C	T_{crit} °C	ρ_l (-20 °C) kg/m³	ρ_v (-20 °C) kg/m³	h_{fg} (-20 °C) kJ/kg
R410A	A1	72.6	-51.4	71.3	1245	15.4	244
R290	A3	44.1	-42.1	96.7	554	5.5	401
Ammonia	B2L	17.0	-33.3	132.4	665	1.6	1329
R600	A3	58.1	0	152	622	1.3	402
R600a	A3	58.1	-11.7	134.7	603	2.1	372
R1270	A3	42.1	-47.6	91.1	574	6.6	406

Four refrigerants were evaluated under the same operating conditions in a simple heat pump model simulated in Dymola/Modelica. The condensation and evaporation temperatures were fixed, and the compression process was assumed ideal. Given the same volume flow rate at the compressor inlet, the volumetric refrigerating effect, pressure ratio, and the effects of subcooling and internal superheating degrees were investigated. As shown in Table 3, ammonia has the highest pressure ratio and COP1 among the studied refrigerants. The volumetric refrigerating effect (Q_v) is the refrigerating capacity of the working fluid achieved per unit volume of vapor drawn into the compressor and decreases with the evaporation temperature. Refrigerants with a high Q_v allow for the use of smaller compressors for a given capacity. This parameter was used to compare refrigerants as it directly indicates the necessary compressor size for a given thermal capacity. To evaluate how sensitive the cycle is to operating parameters, the influence of subcooling and superheating on system performance metrics, such as Q_v and COP, was quantified using y-factors [20]. y_1 denotes the influence of the external subcooling on Q_v and COP. y_2 and y_3 denote the influence of the internal superheating on Q_v and COP, respectively.

$$y_1 = \left(\frac{h_{v,evap,out} - h_{valve,in}}{h_{v,evap,out} - h_{l,cond,out}} - 1\right) \cdot \frac{100}{T_{cond} - T_{valve,in}} \tag{2}$$

$$y_2 = \left(\frac{h_{comp,in} - h_{l,cond,out}}{v_{comp,in}} \cdot \frac{v_{v,evap,out}}{h_{v,evap,out} - h_{l,cond,out}} - 1\right) \cdot \frac{100}{T_{comp,in} - T_{evap}} \tag{3}$$

$$y_3 = \left(\frac{h_{comp,out} - h_{l,cond,out}}{h_{comp,out} - h_{comp,in}} \cdot \frac{h_{is,comp,out} - h_{v,evap,out}}{h_{is,comp,out} - h_{valve,in}} - 1\right) \cdot \frac{100}{T_{comp,in} - T_{evap}} \tag{4}$$

As shown in Table 3, the y-factor values obtained from the Dymola simulations were compared with the reported data for certain refrigerants in [20]. This comparison demonstrates that the Y-factor values are consistent with the previously reported data. Subcooling generally has a positive effect on the system performance; however, this effect is less prominent for Ammonia and more significant for R290. The influence of internal superheat can be positive or negative depending on the refrigerant. For Ammonia, internal superheating has a detrimental impact on the system performance due to the higher specific volume at the compressor inlet which led to increased compression work. In contrast, R290 shows a positive y-factor (0.143%/°C), meaning it benefits from the use of an internal heat exchanger.

Table 3 Cycle analysis of the selected refrigerants (50°C/-20°C)

	P_{cond}	P_{evap}	P_{cond}/P_{evap}	COP_1	Q_v	y_1		y_2		y_3	
	bar	bar	-	-	kJ/m³	%/°C		%/°C		%/°C	
R410A	30.6	3.9	7.69	2.194	1976.30	1.494	1.502*	0.138	0.126*	0.090	0.089*
R290	17.13	2.4	7.00	2.341	1182.79	1.430	1.420*	0.238	0.247*	0.196	0.209*
Ammonia	20.3	1.8	10.73	2.680	1594.81	0.507	0.504*	-0.228	-0.224*	-0.219	-0.213*
R600a	6.8	0.7	9.47	2.454	424.17	1.270	1.274*	0.290	0.288*	0.238	0.255*

* Results from [20]

A comparative analysis was conducted to evaluate natural refrigerants with respect to R410A in a baseline single-stage vapor compression cycle under yearly operating conditions corresponding to MDH requirements. This analysis provided insight into the operating envelope of each refrigerant, including the pressure ratio and suction volume flow rate, and SCOP as a thermodynamic performance measure and an investment cost indicator [24]. Figure 5 (a) illustrates the suction volume flow rate range at the compressor inlet and the pressure ratios at which the cycle operated throughout the year. Due to their low vapor pressure, R600 generally exhibits a low volumetric refrigerating effect, necessitating a relatively larger compressor swept volume to achieve a desired heating capacity at low ambient temperatures. Furthermore, since the evaporation temperature drops to -12 °C at the lowest outdoor air temperature, this refrigerant is considered unsuitable for the current heat pump configuration, therefore it is excluded from the following analysis. The main consequence of ammonia's compression process, led directly to operational challenges characterized by high discharge temperatures, which requires special cycle designs, such as two-stage systems. Figure 5 (b) compares the seasonal performance of the air-source heat pump (ASHP) for different refrigerants across three operating modes: space heating, domestic hot water (DHW), and combined operation. Among the evaluated refrigerants, ammonia demonstrated the highest SCOP in all applications, particularly in DHW mode, reaching nearly 4.0. R290 and R1270 also show favorable performance, with SCOP values for combined operation slightly below that of ammonia. In contrast, R600 and R600a show lower SCOP values across all modes, indicating reduced thermodynamic efficiency. The baseline refrigerant, R410A, shows moderate performance, remaining lower than ammonia and hydrocarbons such as R290 and R1270. Overall, ammonia and R290 stand out as the most efficient options for this heat pump system.

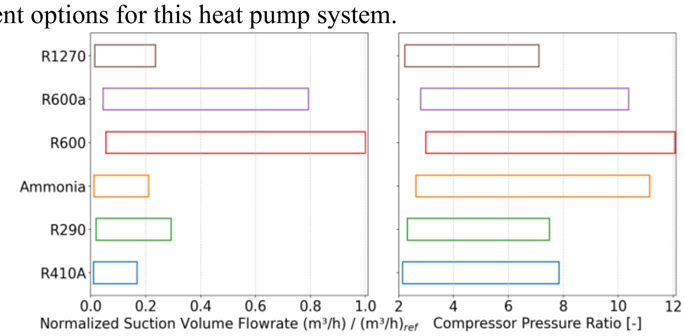

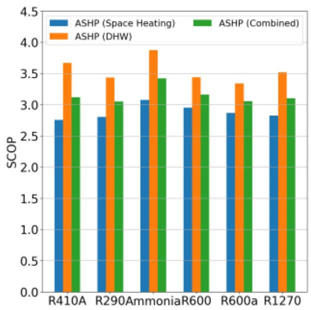

Figure 5 (a) Suction volume flow rate normalized with respect to the maximum value of R600 (a) left and compressor pressure ratio (a) right for various refrigerants. (b) SCOP of the air-source heat pump across different operating modes

The overall objective of this study is to evaluate whether natural refrigerants, such as ammonia and hydrocarbons, could outperform R410A in MDH heat pump applications. Additionally, we wanted to explore whether a dual-source heat pump (DSHP) could improve performance at lower outdoor temperatures by utilizing local heat sources. A comparative analysis is conducted to evaluate the performance of DSHP configuration for various refrigerants, focusing on the contribution of heat sources and identifying the setup that maximized overall efficiency.

The first step involved comparing the performance metrics of the dual-source heat pump with those of a reference air-source heat pump (ASHP). The COP_1 and SCOP were calculated from steady-state simulations, considering different operating conditions. The air source temperature ranged from -3.5 °C to 30 °C, and the secondary heat source temperature ranged from 0 °C (B0) to 25 °C (B25). As shown in Figure 6, the introduction of a secondary heat source in the DSHP increased COP_1 at lower ambient temperatures across all refrigerants. The largest improvement in COP occurred when the secondary source temperature exceeded 15 °C. At this point, DSHP operation resulted in a COP that was 20-30% higher than the baseline ASHP.

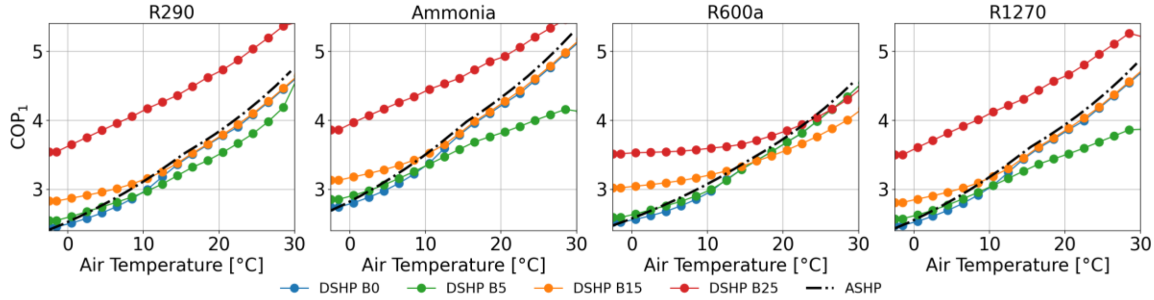

Figure 6 COP variation over the year

Table 4 summarizes the SCOP performance of the air-source heat pump (ASHP) and the percentage improvement achieved by the dual-source configurations. Within each refrigerant, the performance of the DSHP configurations increases with higher secondary-source temperatures. Propane shows consistently higher improvements, starting at 23% for B5 and slightly rising for B15 and 36% for B25. Ammonia also benefits substantially from DSHP operation, with improvements from 24% (B5) up to 32% (B25). R600a shows the smallest improvements overall with SCOP comparable to ASHP performance for B5, only 7% for B15, and 19% for B25, indicating limited benefit from lower-temperature secondary sources. This indicates that DSHP operation is more advantageous when a sufficiently warm secondary source is available. When comparing refrigerants, propane and ammonia show the highest relative improvements across all secondary-source temperatures, followed by R1270.

Table 4 Seasonal Performance of ASHP and Relative SCOP Improvement of DSHP Configurations

Refrigerant	SCOP ASHP	SCOP DSHP (B5) [%]	SCOP DSHP (B15) [%]	SCOP DSHP (B25) [%]
R410A	3.1	16.1	22.6	22.6
Propane	3.1	22.6	29.0	35.5
Ammonia	3.4	23.5	26.5	32.4
R600a	3.1	0.0	6.5	19.4
R1270	3.1	19.4	25.8	32.3

Figure 7 demonstrates the COP distribution as a function of the air-source temperature and the secondary-source temperature. It is apparent that. A higher COP is achieved for all refrigerants at low ambient temperatures when the secondary heat source operates at temperatures above 15 °C. In contrast, for Ammonia the same COP range can be reached when the secondary source temperature exceeds 10 °C. For R600a, the impact of low-temperature secondary sources on COP is relatively subtle when the outdoor temperature exceeds 10 °C and COP generally improves as the ambient temperature rises. The impact on COP is more pronounced at high-temperature secondary sources, particularly for ammonia and R1270. Overall, using a higher-temperature secondary source helps maintain a higher COP.

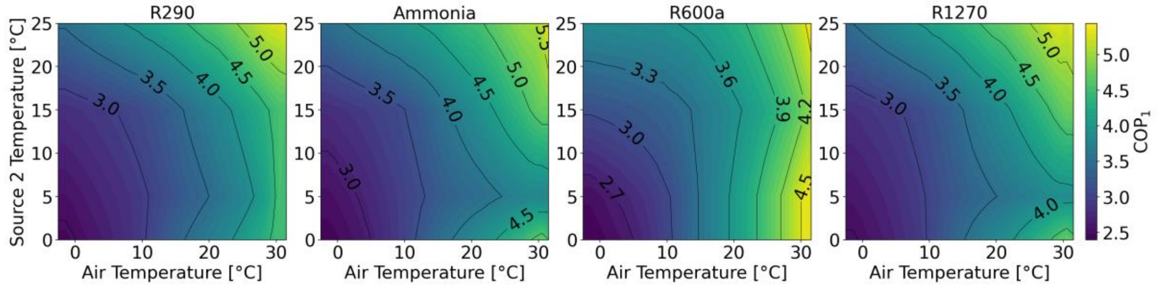

Figure 7 COP distribution in DSHP configuration

Figure 8 shows the distribution of the heat source ratio (β) as a function of the secondary source and ambient temperatures. The higher heat source ratio also reflects an increase in the contribution of the secondary source. As the temperature of the secondary source increased, a larger portion of the cooling demand is met by the second evaporator. This shift to higher-temperature secondary sources contributed to the DSHP's overall efficiency. The COP at low ambient temperatures is reflected in a greater share of the secondary source as the secondary source temperature increases. This means that as the temperature of the secondary source rises, the system becomes more efficient, with a larger portion of the cooling capacity being provided by the second evaporator, particularly at lower ambient temperatures. Additionally, the contribution of the low-temperature secondary heat source to the overall cooling capacity becomes minimal at higher outdoor temperatures.

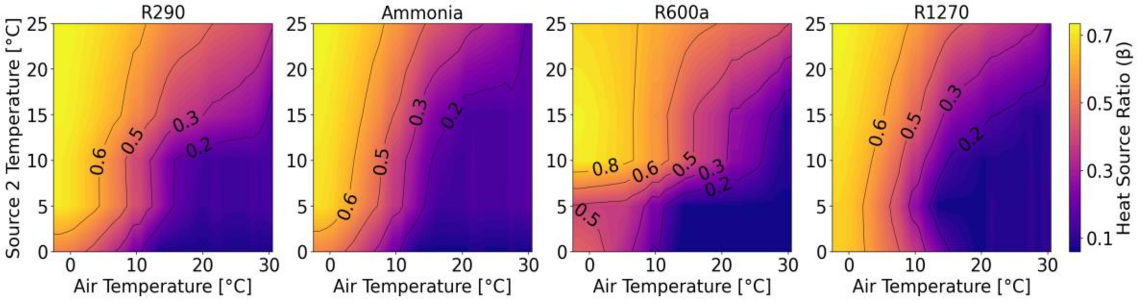

Figure 8 Heat source ratio distribution in DSHP configuration

The performance enhancement achieved through utilizing a secondary heat source in the DSHP comes with added system complexity, including the need for an additional evaporator and compressor. To determine whether the performance improvement justifies these added costs, the compressor power consumption and the overall heat transfer coefficient of the evaporator were analysed. Figure 9 shows that, the total compressor power consumption in a DSHP decreases as the secondary source temperature increases from 15 °C to 25 °C at lower ambient temperatures. The suction-line density at the secondary source is relatively higher than the primary line and the compressor work is proportional to the mass flow rate. Consequently, the shifting refrigerant mass flow towards intermediate evaporator with higher suction density helps the heat pump system to provide the target heating capacity without requiring as much power from the compressor. On the other hand, at lower temperature lifts, the addition of the secondary source may have a less positive impact on total compression work.

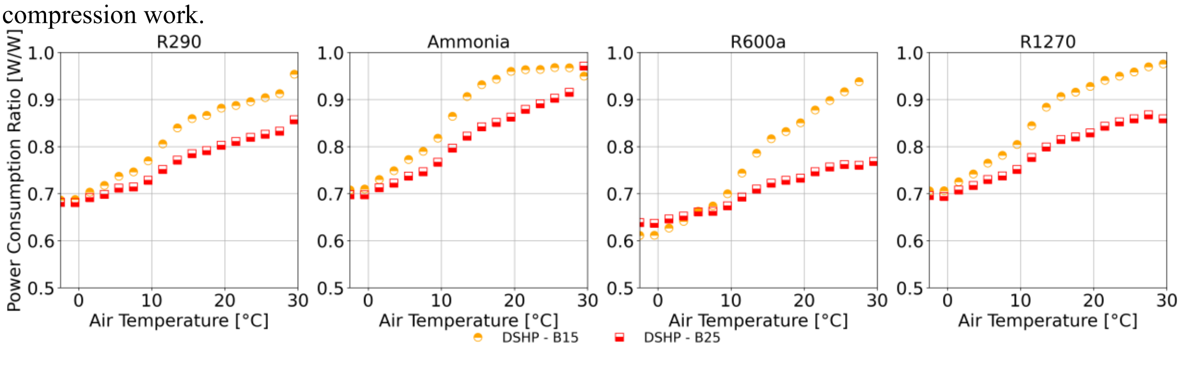

Figure 9 Compressor(s) power consumption ratio in DSHPs B15, and B25.

4. Conclusion

In this study, a thermodynamic evaluation was performed for a heat pump cycle designed to provide space heating and domestic hot water to a MDH network consisting of residential apartment blocks. The dual-source heat pump configuration integrates both ambient air and locally available heat in the urban area as heat sources in parallel. The proposed system was shown to be a competitive alternative to conventional air-source heat pumps, as it enhances energy efficiency and reduces environmental impact.

Numerical simulation results also indicated the potential benefits and viability of using natural refrigerants instead of the commonly used HFC R410A in terms of thermodynamic efficiency. On average, ammonia and R290 achieved SCOP improvements of 32% and 26%, respectively, in DSHP operating modes where the secondary source temperature is above 5 °C, making it a low-GWP working fluid alternative for MDH systems. Additionally, the study showed that a secondary heat source above 15 °C can improve the heat pump's efficiency by increasing the proportion of the cooling capacity met by the second evaporator at higher temperature and pressure.

While the dual-source configuration introduces additional complexity and cost by integrating an extra evaporator and compressor, it significantly improves the COP at lower ambient temperatures. However, it should be noted that a heat pump with the highest COP is not necessarily the best choice for widespread adoption in micro-district heating networks. Overall system performance usually depends on several important factors, including cost, safety, and long-term operational feasibility. Therefore, future analyses should also incorporate cost-related objectives to provide a more comprehensive assessment of energy efficiency, environmental impact, and economic performance. In conclusion, the dual-source heat pump system working with natural refrigerants, such as ammonia and propane, offers a promising and sustainable solution for residential heating demand in densely populated urban areas. These systems can help achieve long-term decarbonization goals.

The study also highlights the importance of refrigerant choice and system configuration in achieving energy efficiency and the EU's carbon neutrality goals by 2050. Further research should explore the long-term economic viability of such systems by taking into account installation and operating costs and potential scalability in different scenarios.

References

[1] Eurostat. "Energy consumption in households." [Online]. Available: https://ec.europa.eu/eurostat/statistics-explained/index.php?title=Energy_consumption_in_households

[2] B. V. Mathiesen, C. Wild, and S. Nielsen, "Heat Matters: The Missing Link in REPowerEU: 2030 District Heating Deployment for a long-term Fossil-free Future," Aalborg Universitet, Copenhagen, 2023.

[3] D. M. Sneum, A. Billerbeck, F. Kachirayil, and R. McKenna, "Barriers to district heating deployment: insights from literature and experts," *Energy Policy*, vol. 206, p. 114780, 2025, doi: 10.1016/j.enpol.2025.114780.

[4] IEA - International Energy Agency, "Tracking Clean Energy Progress 2023," Paris. [Online]. Available: https://www.iea.org/reports/tracking-clean-energy-progress-2023

[5] D. Salite, Y. Miao, and E. Turner, "A comparative analysis of policies and strategies supporting district heating expansion and decarbonisation in Denmark, Sweden, the Netherlands and the United Kingdom – Lessons for slow adopters of district heating," *Environmental Science & Policy*, vol. 161, p. 103897, 2024, doi: 10.1016/j.envsci.2024.103897.

[6] A. Sandvall, M. Hagberg, and K. Lygnerud, "Modelling of urban excess heat use in district heating systems," *Energy Strategy Reviews*, vol. 33, p. 100594, 2021, doi: 10.1016/j.esr.2020.100594.

[7] I. Pakere, M. Feofilovs, K. Lepiksaar, V. Vītoliņš, and D. Blumberga, "Multi-source district heating system full decarbonization strategies: Technical, economic, and environmental assessment," *Energy*, vol. 285, p. 129296, 2023, doi: 10.1016/j.energy.2023.129296.

[8] Euroheat & Power, "DHC Market Outlook 2024," Jun. 2024. [Online]. Available: https://www.euroheat.org/news/dhc-market-outlook-2024-the-most-comprehensive-publication-on-district-heating-and-cooling-to-date-1

[9] R. Conte, M. Tancon, M. Mozafarivanani, E. Zanetti, M. Azzolin, and D. Del Col, "Investigation on a direct expansion multisource carbon dioxide heat pump to maximize the use of renewable energy sources," *Applied Thermal Engineering*, vol. 274, p. 126533, 2025, doi: 10.1016/j.applthermaleng.2025.126533.

[10] S. Siren, J. Hirvonen, and P. Sormunen, "Comparison of traditional and ambient air-assisted ground source heat pump systems using different bore field configurations," *Energy Conversion and Management*, vol. 323, p. 119240, 2025, doi: 10.1016/j.enconman.2024.119240.

[11] G. Besagni, L. Croci, R. Nesa, and L. Molinaroli, "Field study of a novel solar-assisted dual-source multifunctional heat pump," *Renewable Energy*, vol. 132, pp. 1185–1215, 2019, doi: 10.1016/j.renene.2018.08.076.

[12] Z. Han, L. Qu, X. Ma, X. Song, and C. Ma, "Simulation of a multi-source hybrid heat pump system with seasonal thermal storage in cold regions," *Applied Thermal Engineering*, vol. 116, pp. 292–302, 2017, doi: 10.1016/j.applthermaleng.2017.01.057.

[13] G. Emmi, E. Baccega, S. Cesari, E. Mainardi, and M. Bottarelli, "Energy analysis of multi-source heat pump system: A real case study application," *Renewable Energy*, vol. 221, p. 119708, 2024, doi:

10.1016/j.renene.2023.119708.
[14] Y. Wang *et al.,* "Study on performance of a multi-heat source heat pump coupled energy storage system for plant factory heating system," *Energy Conversion and Management*, vol. 319, p. 118917, 2024, doi: 10.1016/j.enconman.2024.118917.
[15] S. Bertsch, M. Uhlmann, and A. Heldstab, "Heat pump with two heat sources on different temperature levels," 2014.
[16] L. Shi, X. Liu, and M. Qu, "Comparison between a residential dual source heat pump system integrated with thermal storage and an air source heat pump system at cold climate," Oak Ridge National Laboratory (ORNL), Oak Ridge, TN (United States).
[17] T. Reum, D. Schmitt, T. Summ, C. Trinkl, F. Ochs, and T. Schrag, "Experimental analysis of parallel operation of two heat sources in a dual-source heat pump incorporating two compressors," *International Journal of Refrigeration*, vol. 171, pp. 124–138, 2025, doi: 10.1016/j.ijrefrig.2024.12.013.
[18] J. A. Fonseca, T.-A. Nguyen, A. Schlueter, and F. Marechal, "City Energy Analyst (CEA): Integrated framework for analysis and optimization of building energy systems in neighborhoods and city districts," *Energy and Buildings*, vol. 113, pp. 202–226, 2016, doi: 10.1016/j.enbuild.2015.11.055.
[19] *EN 15316-4-2:2008 Heating systems in buildings – Method for calculation of system energy requirements and system efficiencies – Part 4-2: Space heating generation systems, heat pump systems.*
[20] E. Granryd, I. Ekroth, P. Lundqvist, Å. Melinder, B. Palm, and P. Rohlin, *Refrigerating engineering*. KTH (Royal Institute of Technology), Department of Energy Technology, Division of applied Thermodynamics and Refrigeration - Sweden/Sweden, 2005.
[21] D. Schmidt *et al.,* "Successful implementation of low temperature district heating case studies," *Energy Reports*, vol. 7, pp. 483–490, 2021, doi: 10.1016/j.egyr.2021.08.079.
[22] B. Zühlsdorf, J. K. Jensen, and B. Elmegaard, "Heat pump working fluid selection—economic and thermodynamic comparison of criteria and boundary conditions," *International Journal of Refrigeration*, vol. 98, pp. 500–513, 2019, doi: 10.1016/j.ijrefrig.2018.11.034.
[23] C. Arpagaus, F. Bless, J. Schiffmann, and S. S. Bertsch, "Multi-temperature heat pumps: A literature review," *International Journal of Refrigeration*, vol. 69, pp. 437–465, 2016, doi: 10.1016/j.ijrefrig.2016.05.014.
[24] C. Höges, L. Wissing, C. Vering, and D. Müller, "How to Choose the Best Refrigerant in Heat Pumps from an Ecologic Perspective? Analyzing the Influence of the Evaluation Method," in *36th International Conference on Efficiency, Cost, Optimization, Simulation and Environmental Impact of Energy Systems (ECOS 2023)*, Las Palmas De Gran Canaria, Spain, J. R. Smith, Ed., 2023, pp. 725–737, doi: 10.52202/069564-0066.
[25] B. Palm, "Hydrocarbons as refrigerants in small heat pump and refrigeration systems – A review," *International Journal of Refrigeration*, vol. 31, no. 4, pp. 552–563, 2008, doi: 10.1016/j.ijrefrig.2007.11.016.
[26] *Refrigerating systems and heat pumps — Safety and environmental requirements: Part 1: Basic requirements, definitions, classification and selection criteria,* ÖNORM EN 378-1, Edition: 2020-12-01.